

TWO-DIMENSIONAL COMPRESSIBLE NAVIER–STOKES FINITE VOLUME COMPUTATIONS BY MEANS OF IMPLICIT SCHEMES

Y. MARX AND J. PIQUET

CFD Group, UA 1217, ENSM, Nantes, France

SUMMARY

A finite volume method for solving the two-dimensional compressible Navier–Stokes equations is presented. Shortcomings of the direct extension to viscous flows of well known methods used for inviscid flows are demonstrated. Nevertheless, the method allows the computation of oscillation-free shocks with only a few iterations. The double-throat GAMM nozzle test case¹ is considered.

KEY WORDS Compressible viscous flows Finite volume Numerical solutions Nozzles Flux splitting Reconstruction Riemann solvers Limiters

INTRODUCTION

The use of second-order TVD upwind schemes is becoming increasingly popular because of their intrinsic damping properties. Moreover, the upwinding leads to diagonally dominant matrices; therefore Gauss–Seidel relaxations can be used to solve unfactored implicit systems.^{2,3} Limitations still remain; some of them are presented in this work which is outlined as follows. First an upwind method used for solving the Navier–Stokes equations with an explicit scheme is briefly described. The implementation of implicit schemes is then presented. Finally, results obtained on the double-throat GAMM nozzle are discussed.

GOVERNING EQUATIONS AND NUMERICAL PROCEDURE

The Navier–Stokes equations written in their two-dimensional conservation form are

$$\frac{\partial U}{\partial t} + \frac{\partial F}{\partial x} + \frac{\partial G}{\partial y} = 0, \quad (1)$$

with $F = F' + F''$ and $G = G' + G''$, where F' and G' are the advective fluxes and F'' and G'' are the diffusive fluxes. Equation (1) is solved with a two-step method. The first step is a local (explicit) approximation of the governing equations and the second step is an implicit correction employed to accelerate the convergence towards a steady state.

At the explicit step the MUSCL approach is followed. This is based on a finite volume approach in which the variables U are assumed to vary linearly in each cell. The piecewise linear distribution $L(u)$ is computed by applying the Harten and Osher⁴ reconstruction. Having calculated the space evolution of the variables U , it remains to solve at the interfaces the Riemann problems arising

from the piecewise distribution. For inviscid problems an efficient way of solving (approximately) these Riemann problems is to use the Van Lee flux vector splitting.⁵ Unfortunately this method cannot be used for viscous problems, at least in the boundary layers.

For an explanation of these difficulties, let us consider the simpler computation of the flow over a flat plate. The Van Leer decomposition normal to the wall is written

$$\frac{\partial G'}{\partial y} = \frac{G'_{j+1}^- - G'_j^-}{\Delta y} + \frac{G'_j^+ - G'_{j-1}^+}{\Delta y}, \quad (2)$$

where $j+1$ is the location of the wall. Now, if j and $j-1$ are sufficiently close to the wall so that $v \simeq 0$, and if the other variables are constant, except the x -velocity component u for which the no-slip condition imposes $u_{j+1} = 0$ (the initial guess commonly used on the flat plate usually satisfies these requirements), the Van Leer decomposition gives

$$\begin{aligned} G'_{j+1}^- &= \left[\frac{-\rho a}{4}, 0, \frac{\rho a^2}{2\gamma}, \frac{-\rho a^3}{2(\gamma^2-1)} \right]_{j+1}^T, \\ G'_j^- &\simeq \left[\frac{-\rho a}{4}, \frac{-\rho a u}{4}, \frac{\rho a^2}{2\gamma}, \frac{-\rho a}{8} \left[u^2 + \frac{4a^2}{\gamma^2-1} \right] \right]_j^T, \\ G'_{j-1}^+ &\simeq \left[\frac{\rho a}{4}, \frac{\rho a u}{4}, P - \frac{\rho a^2}{2\gamma}, \frac{\rho a}{8} \left[u^2 + \frac{4a^2}{\gamma^2-1} \right] \right]_{j-1}^T. \end{aligned} \quad (3)$$

The approximation of (3) for the y -momentum equation leads then to

$$\frac{\partial \rho u v}{\partial y} \simeq \left[\frac{\rho a u}{4\Delta y} \right]_j, \quad (4)$$

which has to be compared with the central difference approximation

$$\frac{\partial \rho u v}{\partial y} \simeq \left[\frac{\rho v u}{2\Delta y} \right]_j. \quad (5)$$

In the approximation (4) the y -velocity v does not appear; thus, if u_j is not small enough, the value of (4) may not be close to zero. From (4) it is clear that the Van Leer decomposition may give poor approximations when applied in a direction normal to a wall. Therefore Riemann solvers able to compute steady contact discontinuities, such as Roe⁶ or Osher⁷ Riemann solvers, must be employed for viscous flows.

IMPLICIT CORRECTION

The role of the implicit correction is to propagate and diffuse the local increment ΔU through the computational domain in order to remove the stability restriction of the explicit approximation. An implicit operator often used results from a time derivation of (1). Approximating implicitly the resulting equation leads to

$$[1 + \Delta t \partial \mathbf{A} / \partial x + \Delta t \partial \mathbf{B} / \partial y] \delta U = \Delta U, \quad (6)$$

where \mathbf{A} and \mathbf{B} are the Jacobians of the fluxes F and G ($\mathbf{A} = \partial F / \partial U$, $\mathbf{B} = \partial G / \partial U$) and ΔU is an explicit approximation of (1).

Factored Coakley scheme

The procedure used by Coakley⁸ starts with a factorization of the operator (6). If only the convective terms are considered, the Jacobians **A** and **B** can be diagonalized:

$$\mathbf{A} = S_x^{-1} \Lambda_x S_x, \quad \mathbf{B} = S_y^{-1} \Lambda_y S_y, \quad (7)$$

where Λ_x and Λ_y are the diagonal matrices of the eigenvalues of **A** and **B**. The system is then 'diagonalized' in the sense of Reference 9, bringing out of the derivatives the terms $S_x^{-1} \Lambda_x$ and $S_y^{-1} \Lambda_y$. Finally, an upwind approximation is performed. Assuming an isotropic diffusion at the implicit step, the resulting scheme is written

$$S_x^{-1} \{ \mathbf{1} + \Delta t \Lambda_x^+ \partial^- / \partial x + \Delta t \Lambda_x^- \partial^+ / \partial x - \Delta t v \partial^2 / \partial x^2 \} S_x \\ \times S_y^{-1} \{ \mathbf{1} + \Delta t \Lambda_y^+ \partial^- / \partial y + \Delta t \Lambda_y^- \partial^+ / \partial y - \Delta t v \partial^2 / \partial y^2 \} S_y \delta U = \Delta U, \quad (8)$$

with $v = \rho^{-1} \max(\mu, \lambda + 2\mu, \gamma\mu/\sigma)$, where σ is the Prandtl number.

Central approximation of the second-order space derivatives and first-order approximation of the first-order derivatives lead to simple tridiagonal matrices at the implicit step. In fact, implicit treatment of the boundaries may reintroduce a coupling between some variables. In order to see the influence of the factorization, an unfactored version of the Coakley scheme was also developed.

Unfactored Coakley scheme

The equivalent of (8) for the unfactored implicit operator is

$$\left\{ \mathbf{1} + \Delta t S_x^{-1} \Lambda_x^+ \frac{\partial^-}{\partial x} S_x + \Delta t S_x^{-1} \Lambda_x^- \frac{\partial^+}{\partial x} S_x - \Delta t S_x^{-1} v \frac{\partial^2}{\partial x^2} S_x + \right. \\ \left. + \Delta t S_y^{-1} \Lambda_y^- \frac{\partial^+}{\partial y} S_y + \Delta t S_y^{-1} \Lambda_y^+ \frac{\partial^-}{\partial y} S_y + \Delta t S_y^{-1} v \frac{\partial^2}{\partial y^2} S_y \right\} \delta U = \Delta U. \quad (9)$$

If (9) is multiplied by S_x , introducing $\delta U^x = S_x \delta U$ and $S = S_y S_x^{-1}$ we get

$$\delta U^x + \Delta t \Lambda_x^+ \frac{\partial^-}{\partial x} \delta U^x + \Delta t \Lambda_x^- \frac{\partial^+}{\partial x} \delta U^x - \Delta t v \frac{\partial^2}{\partial x^2} \delta U^x \\ + \Delta t S^{-1} \Lambda_y^+ \frac{\partial^-}{\partial y} S \delta U^x + \Delta t S^{-1} \Lambda_y^- \frac{\partial^+}{\partial y} S \delta U^x - \Delta t S^{-1} v \frac{\partial^2}{\partial y^2} S \delta U^x = \Delta U. \quad (10)$$

Bringing out of the y -derivatives of the matrices S , one is left with

$$\{ \mathbf{1} + \Delta t \Lambda_x^+ \partial^- / \partial x + \Delta t \Lambda_x^- \partial^+ / \partial x - \Delta t v \partial^2 / \partial x^2 \\ + \Delta t S^{-1} \Lambda_y^+ S \partial^- / \partial y + \Delta t S^{-1} \Lambda_y^- S \partial^+ / \partial y - \Delta t v \partial^2 / \partial y^2 \} \delta U^x = \Delta U. \quad (11)$$

Because of the form (9) of the S and S^{-1} matrices (in a Cartesian mesh),

$$S = \left\| \left\| \begin{array}{cccc} 1 & 0 & 0 & 0 \\ 0 & 1/2\rho a & 0 & -1/2\rho a \\ 0 & \frac{1}{2} & \rho a & \frac{1}{2} \\ 0 & \frac{1}{2} & -\rho a & \frac{1}{2} \end{array} \right\| \right\|, \quad S^{-1} = \left\| \left\| \begin{array}{cccc} 1 & 0 & 0 & 0 \\ 0 & \rho a & \frac{1}{2} & \frac{1}{2} \\ 0 & 0 & 1/2\rho a & -1/2\rho a \\ 0 & -\rho a & \frac{1}{2} & \frac{1}{2} \end{array} \right\| \right\|,$$

the equation for the entropy decouples. With the unfactored scheme it is no longer possible to

invert the matrix of the implicit operator simply with a direct procedure, but as the upwinding leads to a diagonally dominant matrix, iterative methods can be used efficiently. Following Reference 2, a line Gauss-Seidel relaxation is used. Two relaxation sweeps, one in each direction, are needed, but every station needs a 3×3 block-tridiagonal system to be solved and this causes an important increase in computational time. Other types of relaxation have been considered in References 3 and 10.

RESULTS OBTAINED WITH THE IMPLICIT SCHEMES

The method has been tested on the double-throat GAMM nozzle,¹ and similar results to those of the other participants have been obtained. One advantage of the Harten-Osher reconstruction is that the slope of the linear distribution does not automatically vanish at extrema as it does with TVD limiters. This allows computations to be done on coarser grids. For instance, discrepancies between computations on 220×33 and 80×15 grids are almost invisible for the case $Re = 100$.

The implicit schemes allow the computation of steady states similar to those obtained by the explicit scheme, but at a lower computational cost. The history of convergence for the implicit factored Coakley scheme is presented in Figure 1 for different CFL numbers. The CFL number is defined by

$$\Delta t = \text{CFL} \min(\Delta t_x, \Delta t_y),$$

with

$$\Delta t_x = \min_{i,j} \left| \frac{\Delta x}{|u| + a + 4\nu/\Delta x} \right|, \quad \Delta t_y = \min_{i,j} \left| \frac{\Delta y}{|v| + a + 4\nu/\Delta y} \right|,$$

where $v = \max(\mu, \lambda + 2\mu, \gamma\mu/\sigma)$ and σ is the Prandtl number.

A spectacular acceleration of the convergence towards the steady state is obtained with the factored scheme, but for $\text{CFL} = 900$ the residue increases after 250 iterations, leading to a divergence. This phenomenon is due to the factorization, which induces an error proportional to the product of the CFL numbers in the x - and y -directions. Using the non-factored Coakley scheme, higher CFL numbers can be utilized, but, unless a more complete treatment of the viscous derivatives at the implicit step is carried out,¹⁰ no improvement in the convergence rate is

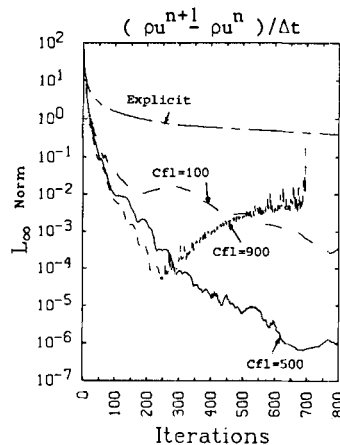


Figure 1. History of convergence for the implicit factored Coakley scheme; $Re = 100$

obtained (Figure 2). As a result of the inherent non-linearity of the reconstruction, periodic oscillations in the convergence curve are set up (Figure 3). When the first-order scheme (constant distribution within each cell) is used, the machine accuracy can be reached, at least at $CFL = 50$ (Figure 4). For higher CFL numbers a sudden change in the slope appears after 1400 iterations. An inspection of the residuals shows that their highest values are of high frequency; they are generated locally by the wall and the exit boundary.

Unfortunately, high-frequency components of the error are badly damped out by the factored Coakley scheme¹¹ when large values of Δt are used. For smaller Δt the damping properties of the scheme become better at high frequencies. Therefore, if a small CFL number is used just after the sudden change in the slope, an increased convergence rate must be found. This is indeed verified (Figure 5), but one can observe also that once the scheme has damped the high frequencies efficiently, a new change occurs in the slope. Again the low frequencies dominate the error and the CFL number has to be increased to improve the convergence rate again. In summary, in contradiction to what was found in References 3 and 12, it is difficult to say that the best

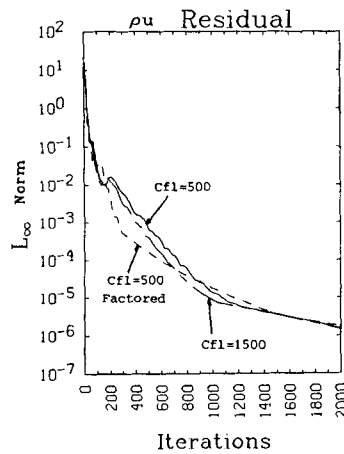


Figure 2. History of convergence for the unfactored first-order scheme; $Re = 100$

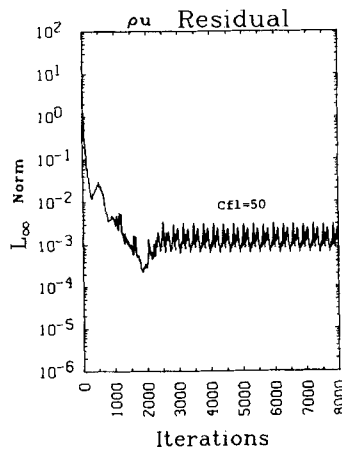


Figure 3. History of convergence for the implicit factored Coakley scheme; $Re = 100$

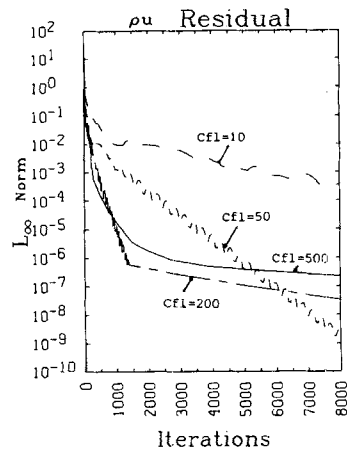


Figure 4. History of convergence for the factored first-order scheme; $Re = 100$

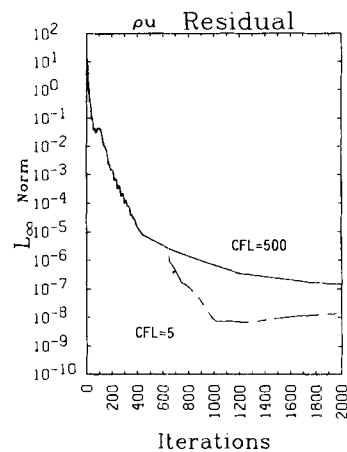


Figure 5. History of convergence for the factored first-order scheme, with modification of the CFL number for damping the high frequencies; $Re = 100$

convergence rate results from an optimal time step existing for the factored implicit scheme. But, *for one given range of the dominant error frequencies, such an optimal time step exists.*

Therefore the most natural procedure for increasing the convergence rate is to use a CFL number which varies with the iterations. Such a procedure has been developed and the resulting convergence history is presented in Figure 6. The CFL number is computed from an estimation of the slope of the convergence curve. When the slope increases, the CFL number is tentatively changed (e.g. decreased), but if this change does not increase the convergence, it is reversed (i.e. the CFL will be increased). With this procedure, which could be further improved, the residual is lowered to machine zero in about 2000 iterations.

It has also been verified that, for the first-order scheme, the implicit correction leads to steady states which do not depend on the time steps. Such a verification is difficult to perform for second-order schemes because of the limiting cycle behaviour.

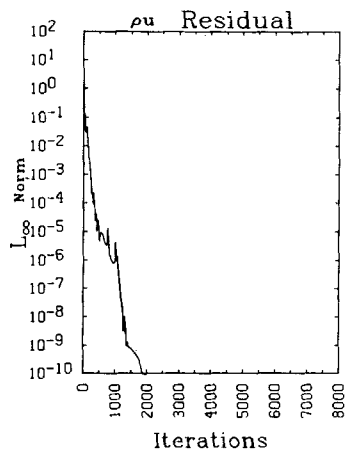


Figure 6. History of convergence for the factored first-order scheme, with variable CFL number; $Re = 100$

CONCLUSIONS

The use of implicit upwind methods allows an important convergence acceleration. The superiority of using a varying time step instead of a constant time step has been demonstrated. The procedure of a self-adjusting CFL number avoids the need for *a priori* knowledge of some 'optimal' CFL number which was often reported for factorized implicit schemes. Another possibility of increasing the convergence is to use implicit schemes as a relaxation scheme in a multigrid procedure.¹¹

ACKNOWLEDGEMENTS

This study was started with the help of CNRS (ATP 9.84.69). Financial support of DRET through contract 86.34.107 is gratefully acknowledged. Computations have been performed on the NAS 9080 and on the VP200 (CIRCE), and with a donation of 20 h on the Cray 1S (CCVR) by the Scientific Committee of the CCVR.

REFERENCES

1. M. O. Bristeau, R. Glowinski, J. Périaux and H. Viviand (eds), 'Numerical simulation of compressible Navier-Stokes equations', *Proc. Gamm Workshop, Notes on Numerical Fluid Dynamics, Vol. 17*, Vieweg-Verlag, 1986.
2. R. W. Mac Cormack, 'Current states of numerical solutions of the Navier-Stokes equations', *AIAA Paper 85-0360*, 1985.
3. J. L. Thomas, B. Van Leer and R. W. Walters, 'Implicit flux-split schemes for the Euler equations', *AIAA Paper 85-1680*, 1985.
4. A. Harten and S. Osher, 'Uniformly high-order accurate non oscillatory schemes I', *NASA CR 175768*, June 1985.
5. B. Van Leer, 'Flux-vector splitting for the Euler equations', in *Lecture Notes in Physics Vol. 170*, Springer-Verlag, 1982, pp. 507-511.
6. P. L. Roe, 'Approximate Riemann solvers, parameter vectors and difference schemes', *J. Comput. Phys.*, **43**, 357-372 (1981).
7. S. Osher, 'Shock modelling in aeronautics', in *Numerical Methods for Fluid Dynamics*, Academic Press, 1982, pp. 179-217.
8. T. J. Coakley, 'Numerical method for gas dynamics combining characteristic and conservation concepts', *AIAA Paper 81-1257*, 1981.
9. D. S. Chaussee and T. H. Pulliam, 'A diagonal form of an implicit approximate factorization algorithm with application to a two-dimensional inlet', *AIAA Paper 80-0067*, 1980.

10. Y. Marx and J. Piquet, 'Comparison of implicit methods for the compressible Navier–Stokes equations', *ICFD Conf., Oxford*, in *Numerical Methods for Fluid Dynamics III*; K. W. Morton, (ed.), Clarendon Press, Oxford, 1988.
11. Y. Marx and J. Piquet, 'Towards multigrid acceleration of 2D compressible Navier–Stokes finite volume implicit schemes', *4th GAMM Seminar on 'Robust Multigrid Methods'*; W. Hackbusch (ed.), Vieweg–Verlag, 1988.
12. W. T. Thompkins and R. H. Bush, 'Boundary treatments for implicit solutions to Euler and Navier–Stokes equations', *J. Comput. Phys.*, **48**, 302–311 (1982).